



Since January 2020 Elsevier has created a COVID-19 resource centre with free information in English and Mandarin on the novel coronavirus COVID-19. The COVID-19 resource centre is hosted on Elsevier Connect, the company's public news and information website.

Elsevier hereby grants permission to make all its COVID-19-related research that is available on the COVID-19 resource centre - including this research content - immediately available in PubMed Central and other publicly funded repositories, such as the WHO COVID database with rights for unrestricted research re-use and analyses in any form or by any means with acknowledgement of the original source. These permissions are granted for free by Elsevier for as long as the COVID-19 resource centre remains active.



Polymeric and lipid nanoparticles for delivery of self-amplifying RNA vaccines

Anna K. Blakney^{a,b,*}, Paul F. McKay^b, Kai Hu^b, Karnyart Samnuan^b, Nikita Jain^c, Andrew Brown^c, Anitha Thomas^c, Paul Rogers^b, Krupal Polra^b, Hadijatou Sallah^b, Jonathan Yeow^d, Yunqing Zhu^{d,e}, Molly M. Stevens^d, Andrew Geall^c, Robin J. Shattock^{b,*}

^a The University of British Columbia, Michael Smith Laboratories, School of Biomedical Engineering, Vancouver, BC V6T1Z4, Canada

^b Imperial College London, Department of Infectious Disease, London W21PG, United Kingdom

^c Precision NanoSystems Inc., Vancouver, BC V6P6T7, Canada

^d Imperial College London, Department of Materials, Department of Bioengineering, Institute of Biomedical Engineering, London SW72BU, United Kingdom

^e School of Materials Science and Engineering, Tongji University, Shanghai 200092, China

ARTICLE INFO

Keywords:

Self-amplifying RNA
Replicon
Vaccine
Polyplex
Lipid nanoparticle
Protein expression
Immunogenicity
SARS-CoV-2

ABSTRACT

Self-amplifying RNA (saRNA) is a next-generation vaccine platform, but like all nucleic acids, requires a delivery vehicle to promote cellular uptake and protect the saRNA from degradation. To date, delivery platforms for saRNA have included lipid nanoparticles (LNP), polyplexes and cationic nanoemulsions; of these LNP are the most clinically advanced with the recent FDA approval of COVID-19 based-modified mRNA vaccines. While the effect of RNA on vaccine immunogenicity is well studied, the role of biomaterials in saRNA vaccine effectiveness is under investigated. Here, we tested saRNA formulated with either pABOL, a bioreducible polymer, or LNP, and characterized the protein expression and vaccine immunogenicity of both platforms. We observed that pABOL-formulated saRNA resulted in a higher magnitude of protein expression, but that the LNP formulations were overall more immunogenic. Furthermore, we observed that both the helper phospholipid and route of administration (intramuscular *versus* intranasal) of LNP impacted the vaccine immunogenicity of two model antigens (influenza hemagglutinin and SARS-CoV-2 spike protein). We observed that LNP administered intramuscularly, but not pABOL or LNP administered intranasally, resulted in increased acute interleukin-6 expression after vaccination. Overall, these results indicate that delivery systems and routes of administration may fulfill different delivery niches within the field of saRNA genetic medicines.

1. Introduction

Self-amplifying RNA (saRNA) is a next-generation platform for nucleic acid vaccines [1]. The backbone, typically derived from an alphaviral genome [2], encodes a gene of interest (GOI) and a viral replicase, which is able to amplify the genomic and subgenomic RNA. The self-amplification properties enable use of a much lower dose of saRNA compared to messenger RNA (mRNA), typically 100-fold lower [3]. saRNA is a versatile platform since it is possible to generate a vaccine against any pathogen for which a protein target is known, for example, influenza [4], chlamydia [5], HIV-1 [6,7], Ebola [8] and RSV [9]. Furthermore, the potential of saRNA was recently tested in a first-in-human combined Phase I/II clinical trial against SARS-CoV-2, demonstrating the potency and scalability of this technology [1,10]. Like all

nucleic acid vaccines and therapies, saRNA requires a delivery vehicle to promote cellular uptake and inhibit degradation of the RNA.

Previous formulations of saRNA have been primarily lipid nanoparticles (LNP) [5,6,10,11], polyplexes [4,8] and cationic nanoemulsions [7]. LNP are the most clinically progressed formulation technology for both saRNA and mRNA, with the recent Emergency Use Authorization of the Pfizer/BioNTech [12] and Moderna [13] COVID-19 vaccines, which are both LNP formulations. Typically, LNP formulations contain an ionizable lipid, helper lipids (cholesterol and a phospholipid) and a PEGylated lipid [14]. While the saRNA is typically encapsulated on the interior of the LNP, it has also been shown that the saRNA can be complexed to the exterior of an LNP in a lipoplex [6]. Although various formulations have been shown to be effective platforms for saRNA, there have been few head-to-head studies comparing the delivery efficiency

* Corresponding authors at: Imperial College London, Department of Infectious Disease, London W21PG, United Kingdom.

E-mail addresses: anna.blakney@msl.ubc.ca (A.K. Blakney), r.shattock@imperial.ac.uk (R.J. Shattock).

<https://doi.org/10.1016/j.jconrel.2021.08.029>

Received 12 April 2021; Received in revised form 12 August 2021; Accepted 16 August 2021

Available online 18 August 2021

0168-3659/© 2021 The Author(s).

Published by Elsevier B.V. This is an open access article under the CC BY-NC-ND license

(<http://creativecommons.org/licenses/by-nc-nd/4.0/>).

and vaccine immunogenicity of these systems.

It is well known that RNA is detected by innate intracellular sensing mechanisms, such as toll-like receptors (TLR) 3, 7 and 8, retinoic acid-inducible gene I (RIG-I), protein kinase R (PKR) and 2'-5' oligoadenylate synthetase (OAS) [15,16]. This innate sensing is known to elicit the self-adjuvantation properties of RNA vaccines [17], but can also inhibit translation [18] and lead to upregulation of mRNA degradation [19]. Beyond RNA sensing, Miao et al. observed that LNP formulations with a dihydroimidazole linker, cyclic amine head group and unsaturated lipid tail target the intracellular stimulator of interferon genes (STING) pathway, resulting in limited cytokine expression and enhanced anti-tumor efficacy. Furthermore, the route of administration is known to affect the protein expression from mRNA formulations [20], although the protein expression is not necessarily correlated with vaccine immunogenicity [4]. The role of the delivery vehicle, and how this varies between formulations and routes of administration, in saRNA protein expression and vaccine immunogenicity has not previously been investigated.

Here, we performed a head-to-head comparison of saRNA formulated with LNP or pABOL, a bioreducible polymer that was previously shown to be an efficient delivery vehicle for saRNA vaccines [4]. We first compared the *in vivo* protein expression of saRNA formulated with pABOL and a variety of LNP formulations. We then compared the matching formulations with saRNA encoding the influenza hemagglutinin (HA) glycoprotein as a model antigen in order to characterize immunogenicity differences. Furthermore, we also investigated the dose response curve for LNP against the spike glycoprotein protein from SARS-CoV-2 as a model antigen and compared the intramuscular (IM) and intranasal (IN) routes of administration. We characterized the humoral immune responses, including circulating and mucosal antibody titers and viral neutralization, as well as cellular immunity. Finally, we assessed differences in systemic cytokine responses arising due to

variations in formulation and route of administration.

2. Materials and methods

2.1. Vectors

saRNA was synthesized from a backbone plasmid vector based on a Trinidad donkey Venezuelan equine encephalitis strain (VEEV) alpha-virus genome as previously described (Fig. 1A) [21]. The gene of interest (GOI) for *in vivo* protein quantification studies was firefly luciferase (fLuc) and either hemagglutinin from the H1N1 A/California/07/2009 strain [4] or the spike glycoprotein of severe acute respiratory syndrome coronavirus 2 (SARS-CoV-2) [21] for *in vivo* immunogenicity studies. Plasmid DNA (pDNA) was transformed into DH5α *E. coli* (New England BioLabs, UK), cultured in 100 mL of Luria Broth (LB) with 100 µg/mL carbenicillin (SigmaAldrich, UK) and isolated using a Plasmid Plus MaxiPrep™ kit (QIAGEN, UK). The concentration of pDNA was measured on a NanoDrop One™ (ThermoFisher, UK).

2.2. *In vitro* transcription of saRNA

Post-transcriptionally capped saRNA was synthesized as previously described [11]. Briefly, uncapped RNA was prepared using 1 µg of linearized DNA template in a MEGAScript reaction (Ambion, UK) according to the manufacturer's protocol. Transcripts were then purified by overnight LiCl precipitation at –20 °C, pelleted by centrifugation at 14,000 RPM for 20 min at 4 °C, washed once with 70% ethanol, centrifuged at 14,000 RPM for 5 min at 4 °C and then resuspended in UltraPure H₂O (Ambion, UK). Purified transcripts were then capped using the ScriptCap m⁷G capping system (CellScript, Madison, WI, USA) and ScriptCap 2'-O-methyltransferase kit (CellScript) simultaneously according to the manufacturer's protocol. Capped transcripts were then

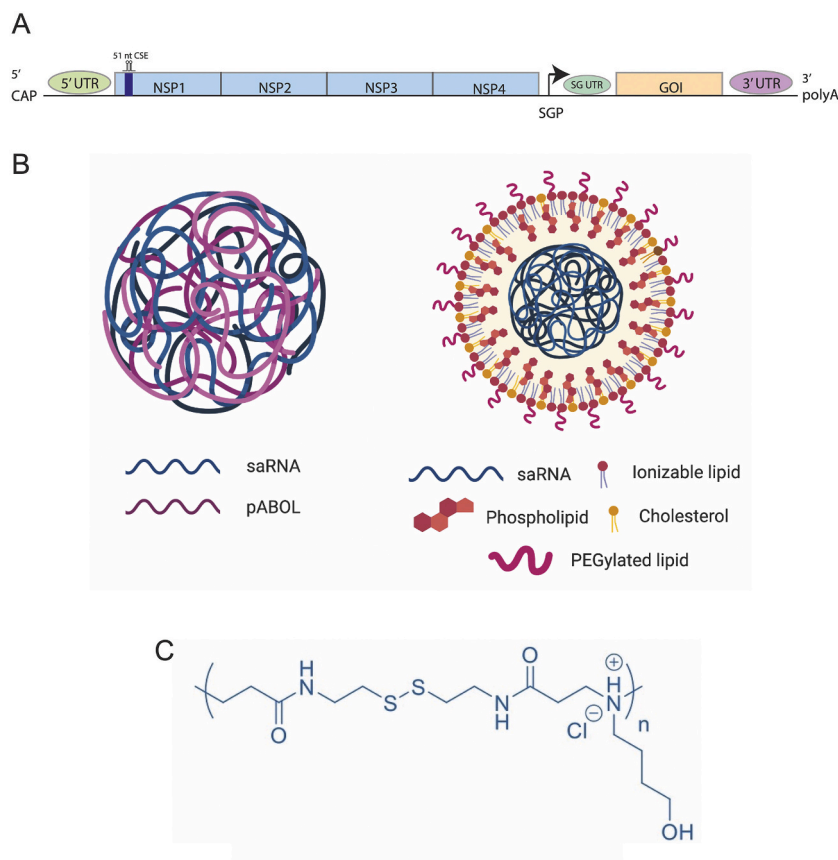


Fig. 1. Schematic illustration of VEEV self-amplifying RNA (A), polymeric and lipid nanoparticle formulations (B) and pABOL chemical structure (C).

purified by LiCl precipitation, as detailed above, resuspended in Ultra-Pure H₂O and stored at –80 °C until formulation.

2.3. saRNA formulation with pABOL

pABOL ($M_w = 8$ kDa) was prepared using a modified literature protocol [4]. *N,N'*-cystaminebis(acrylamide) (CBA) (1.855 g, 7.12 mmol), 4-amino-1-butanol (ABOL) (654.7 μ L, 7.10 mmol), and triethylamine (98.2 μ L, 0.705 mmol) were added into a Schlenk flask charged with a stir bar. A mixed solvent, MeOH/water (1.469 mL, 4/1, v/v), was subsequently added. Polymerization was carried out in the dark at 45 °C under a static nitrogen atmosphere. Aliquots of the reaction mixture were taken until the weight average molecular weight reached 8 kDa according to GPC analysis using narrow PMMA standards and DMF as eluent. The reaction was subsequently quenched by the addition of 10% excess ABOL (65.4 μ L, 0.710 mmol) and allowed to stir at 45 °C for an additional 24 h. The reaction mixture was then diluted with MeOH, acidified with 1 M HCl to pH ~ 4, and then purified by dialysis against acidic water (pH ~ 4, refreshed twice daily over 7 days). The polymers in their HCl-salt form were collected as a white solid after lyophilisation. A stock solution of 8 kDa pABOL was prepared in molecular grade water at a concentration of 50 mg/mL. Polyplexes were prepared by the 'titration method' as previously described [4]. Briefly, in a typical preparation, 5 μ L of a stock solution of saRNA (1 mg/mL) was diluted in 35 μ L of HEPES buffer (20 mM HEPES, 5 wt% glucose in water, pH 7.4). A volume of 4.5 μ L of pABOL stock solution was diluted in 5.5 μ L of HEPES buffer. The saRNA solution was then added to the polymer solution (mixed at 1200 RPM) at a rate of 160 μ L/min, for a final N:P ratio of 45:1.

2.4. saRNA formulation with LNP

A proprietary mix of lipids was prepared at a concentration of 25 mM in ethanol, including an ionizable lipid (Precision NanoSystems, Inc.), helper lipid (either 1,2-dioleoyl-sn-glycero-3-phosphoethanolamine (DOPE) or 1,2-distearoyl-sn-glycero-3-phosphocholine (DSPC), cholesterol and 1,2-dimyristoyl-rac-glycero-3-methoxypolyethylene glycol-2000 DMG-PEG) as detailed in patent publication WO21000041 A1. saRNA was diluted to a concentration of 174 μ g/mL in RNA formulation buffer at pH 4. Lipids in ethanol and saRNA in aqueous buffer were mixed to form lipid nanoparticles on a NanoAssemblr® Ignite™ at an N:P ratio of 8:1, a flow rate ratio of 3:1 (RNA to lipids), total flow rate of 12 mL/min and start waste volumes of 0.05 mL. The LNP were then diluted 40 \times in 1 \times PBS (Ca²⁺ and Mg²⁺ free) and centrifuged using an Amicon ULTRA-15 10,000 MWCO centrifugal filter (Millipore, UK) at 2000 \times g for 30 min at 10 °C to remove ethanol.

2.5. Nanoparticle characterization

Particle size (hydrodynamic diameter, D_h) and polydispersity (\mathcal{D}) was analyzed using dynamic light scattering (DLS) and measured on a Zetasizer Nano ZS™ instrument (Malvern, UK). The scattering angle was fixed at 173° and data was processed using cumulant analysis of the experimental correlation function, and the Stokes-Einstein equation to calculate hydrodynamic radii. Zeta potential measurements were also conducted at 25 °C on a Zetasizer Nano ZS instrument. All solutions were analyzed using disposable polystyrene cuvettes.

2.6. Encapsulation efficiency

The encapsulation efficiency of LNP were quantified using a modified RiboGreen assay (Life Technologies, UK). 1 \times TE buffer was prepared by adding 10 mL of 20 \times TE buffer to 190 mL RNase-free water. Triton buffer was prepared by adding 2 mL of Triton X-100 to 100 mL of 1 \times TE buffer. Stock solutions of RNA and samples were prepared in Triton buffer, and the assay was performed according to the

manufacturer's protocol in a black 96 well plate. The plate was analyzed using a FLUOstar Omega™ plate reader (BMG LABTECH, UK) using an excitation of 485 nm and emission of 528 nm, and the background fluorescence was subtracted from each sample during analysis. The encapsulation efficiency (EE) was calculated using the following equation:

$$EE = 100 \times \frac{\text{Total RNA}_{\text{RiboGreen in Triton TE buffer}} - \text{RNA outside LNP}_{\text{RiboGreen in TE}}}{\text{Total RNA}_{\text{RiboGreen in Triton TE buffer}}}$$

2.7. In vivo fluc expression in mice

All animals were handled in accordance with the UK Home Office Animals Scientific Procedures Act 1986 and with an internal ethics board (the Animal Welfare and Ethical Review Body (AWERB)), and UK government approved project license (P63FE629C) and personal license (IC37CBB8F). Food and water were supplied *ad libitum*. Female BALB/c mice (Charles River, UK) 6–8 weeks of age were placed into groups ($n = 5$) and housed in a full acclimatized room. *In vivo* imaging was performed as previously described [5]. Mice were injected intramuscularly (IM) in both hind leg quadriceps with 5 μ g of fluc saRNA formulations in a total volume of 50 μ L. After 7 days, the mice were injected intraperitoneally (IP) with 150 μ L of XenoLight RediJect™ D-Luciferin substrate (PerkinElmer, UK) and allowed to rest for 10 min. Mice were then anesthetized using isoflurane and imaged on an *In Vivo* Imaging System (IVIS) FX Pro™ (Kodak Co., Rochester, NY, USA) equipped with Molecular Imaging software version 5.0 (Carestream Health, USA) for 2 min. The signal from each injection site was quantified using Molecular Imaging software and expressed as total flux (p/s).

2.8. In vivo HA and SARS-CoV-2 immunogenicity in mice

BALB/c mice aged 6–8 weeks old were placed into groups of $n = 5$ and injected intramuscularly in the hind quadriceps with a dose of HA or SARS-CoV-2 saRNA formulated with LNP or pABOL, ranging in doses from 0.0001 to 1 μ g of RNA in a volume of 50 μ L. For intranasal (IN) administration, mice were anesthetized using isoflurane and formulations were pipetted into the nasal cavity in a volume of 100 μ L. Animals were immunized at week 0, boosted with a second vaccination at week 4 and either challenged or euthanized using a Schedule 1 method at week 6, at which time the spleens were excised and processed into single cell suspensions for use in assays. Serum samples were collected at week 4 and 6 timepoints. Mucosal sampling was performed at week 6 by rinsing the vaginal cavity with a positive displacement pipette with a total of 150 μ L of PBS per mouse.

2.9. Influenza challenge study

Two weeks after the boost injection (6-week timepoint), mice were challenged with 4.2×10^5 pfu of influenza (Cal/09) suspended in 100 μ L of PBS. Mice were anesthetized using isoflurane and challenged IN. Mice were weighed individually each day to determine weight loss. According to the challenge protocol human endpoint, mice were euthanized if they sustained more than 3 days of 20% weight loss or 1 day of 25% weight loss in line with the humane endpoints detailed in the animal license.

2.10. HA and SARS-CoV-2 specific ELISA

A semi-quantitative immunoglobulin ELISA protocol was performed as previously described for HA and SARS-CoV-2 spike antigens. [22] MaxiSorp™ high binding ELISA plates (Nunc, UK) were coated with 100 μ L per well of 1 μ g/mL recombinant HA or SARS-CoV2 protein in PBS. For the standard, three columns on each plate were coated with 1:1000 dilutions of both goat anti-mouse Kappa (Southern Biotech) and Lambda light chains (Southern Biotech). After overnight incubation at 4 °C, the plates were washed 4 \times with 0.05% (v/v) Tween-20 in PBS and blocked

for 1 h at 37 °C with 200 µL of blocking buffer (1% BSA (w/V) in 0.05% (v/v) Tween-20 in PBS). The plates were washed and the diluted samples or a 5-fold dilution series of the standard IgG was added in a volume of 50 µL per well. Plates were incubated for 1 h at 37 °C, washed and the secondary antibody (anti-mouse IgG-HRP, Southern Biotech) was added at a 1:2000 dilution in blocker buffer. After incubation at 37 °C for 1 h the plates were washed and developed using 50 µL per well SureBlue TMB (3,3', 5,5'-tetramethylbenzidine) substrate, and the reaction stopped after 5 min with 50 µL of stop solution (Insight Biotechnologies) per well. The absorbance was read on a Versamax Spectrophotometer at 450 nm (BioTek Industries).

2.11. Pseudotyped virus neutralization assay

An HIV-pseudotyped luciferase-reporter based system was used to assess the neutralization ability of sera from vaccinated animals against SARS-CoV-2 as previously described [21]. Briefly, the SARS-CoV-2 pseudotyped virus was produced by co-transfection of HEK 293 T.17 cells with an HIV-1 *gag-pol* plasmid (pCMV-Δ8.91, a kind gift from Prof. Julian Ma, St George's University of London), a firefly luciferase reporter plasmid (pCSFLW, a kind gift from Prof. Julian Ma, St George's University of London) and a plasmid encoding the S protein (pSARS-CoV2-S) at a ratio of 1:1.5:1. Virus-containing medium was clarified by centrifugation and filtered through a 0.45 µm membrane 72 h after transfection, aliquoted and stored at –80 °C. For the neutralization assay, heat-inactivated sera were first serially diluted and incubated with virus for 1 h, then the serum-virus mixture was transferred into wells pre-seeded with Caco2 cells. After 48 h cells were lysed, and luciferase activity was measured using the Bright-Glo™ Luciferase Assay (Promega, UK). The neutralization IC₅₀ was then calculated using GraphPad Prism™ (version 8.4).

2.12. IFN-γ ELISpots

Quantification of the IFN-γ T cell response was performed using the Mouse IFN-γ ELISpot^{PLUS} kit (Mabtech) according to the manufacturer's protocol. Briefly, anti-IFN-γ pre-coated plates were blocked with DMEM +10% FBS for at least 30 min, then splenocytes were added at 2.5×10^5 cells per well for negative control (media only) and SARS-CoV-2 peptide pools (15-mers overlapping by 11; JPT Peptides) (1 µg/mL) in a volume of 200 µL per well. The positive control wells contained 5×10^4 splenocytes per well in a 200 µL volume per well with a concentration of 5 µg/mL of ConA. Plates were incubated overnight with 5% CO₂ in a 37 °C incubator and developed per the manufacturer's protocol. Once dried, plates were read using the AID ELISpot reader ELR03 and READER software (Autoimmun Diagnostika GmbH).

2.13. Cytokine analysis in sera

Mice were bled 4 h after inoculation with SARS-CoV-2 LNP or pABOL formulations and the sera was collected and stored at –80 °C. The cytokine response was characterized using a Mouse Th1/Th2 ProcartaPlex Immunoassay (ThermoFisher Scientific, UK) on a Bio-Plex 200 System (Bio-Rad), according to the manufacturer's instructions.

2.14. Statistical analysis

Graphs and statistical analysis were prepared in GraphPad Prism (version 9). Statistical differences were analyzed using either a two-way ANOVA adjusted for multiple comparisons or a Kruskal-Wallis test adjusted for multiple comparisons, with $p < 0.05$ used to indicate significance.

3. Results

3.1. pABOL and LNP formulations exhibit similar size and encapsulation efficiency, but not surface charge

The physical characterization of saRNA formulations prepared with LNP or pABOL (Table 1, Fig. 1B) is shown in Fig. 2. The particle diameters and polydispersity for pABOL (Fig. 1C), DOPE (LM01-04PE) and DSPC (LM03PC) LNP formulations were equivalent; ~80 nm for all particles with polydispersity of ~0.10 (Fig. 2A). However, there were differences in the surface charge (zeta potential) between the pABOL and LNP formulations. The pABOL polyplexes, formulated at a previously optimized N:P ratio of 45:1, [4] had a positive zeta potential of +8 mV, whereas the LNP formulations had a neutral zeta potential (–2 to +2 mV) (Fig. 2B). Quantification of encapsulated (LNP) or complexed (pABOL) saRNA revealed that all formulations had high encapsulation efficiency (>84%, Fig. 2C). Overall, the nanoparticles exhibited similar size and encapsulation efficiency, but pABOL formulations had a more positive surface charge than LNP.

Table 1
Lipid nanoparticle formulation compositions.

ID	Ionizable lipid	Phospholipid	Lipid mole ratio (Ionizable lipid: phospholipid: cholesterol: DMG-PEG)	N/P Ratio
LM01PE	(2R,3S,4S)-2-(((4-(dimethylamino)butanoyloxy)methyl)tetrahydrofuran-3,4-diyl (9Z,9'Z,12Z,12'Z)-bis(octadeca-9,12-dienoate)	DOPE	50:10:38.5:1.5	8
LM02PE	(2R,3S,4S)-2-(((5-(dimethylamino)pentanoyloxy)methyl)tetrahydrofuran-3,4-diyl (9Z,9'Z,12Z,12'Z)-bis(octadeca-9,12-dienoate)	DOPE	50:10:38.5:1.5	8
LM03PE	(2R,3S,4S)-2-(((1,4-dimethylpiperidine-4-carbonyloxy)methyl)tetrahydrofuran-3,4-diyl (9Z,9'Z,12Z,12'Z)-bis(octadeca-9,12-dienoate)	DOPE	50:10:38.5:1.5	8
LM04PE	(2R,3S,4S)-2-(((1,3-dimethylpyrrolidine-3-carbonyloxy)methyl)tetrahydrofuran-3,4-diyl (9Z,9'Z,12Z,12'Z)-bis(octadeca-9,12-dienoate)	DOPE	50:10:38.5:1.5	8
LM03PC	(2R,3S,4S)-2-(((1,4-dimethylpiperidine-4-carbonyloxy)methyl)tetrahydrofuran-3,4-diyl (9Z,9'Z,12Z,12'Z)-bis(octadeca-9,12-dienoate)	DSPC	50:10:38.5:1.5	8

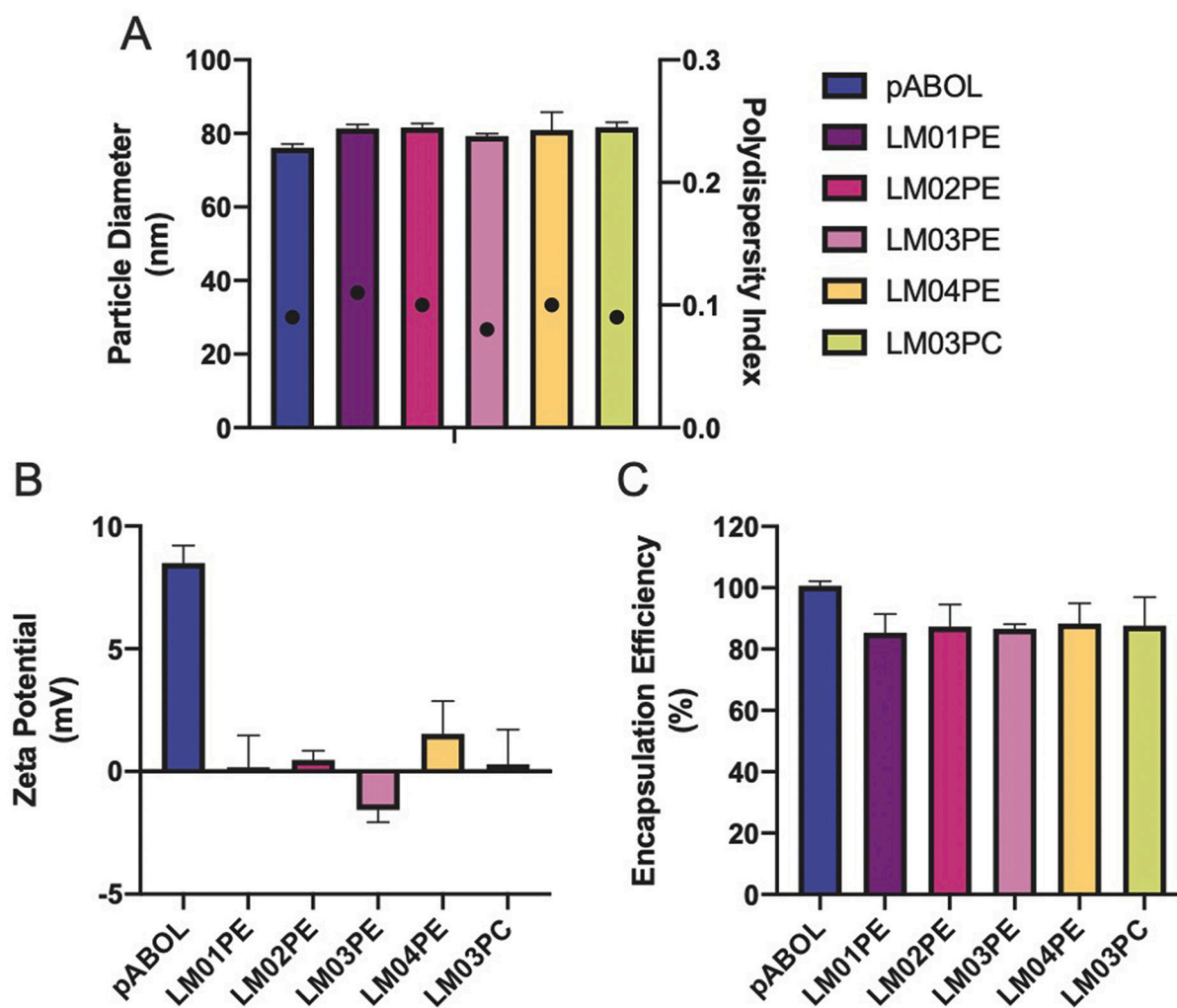


Fig. 2. Characterization of saRNA polymeric and lipid nanoparticle formulations: particle size (A) and zeta potential (B) as determined by dynamic light scattering (DLS) and encapsulation efficiency of saRNA relative to initial loading (C) as determined by RiboGreen assay. Bars represent mean \pm standard deviation for $n = 3$. For (A), bars and error bars correspond to the left axis (particle diameter) and dots correspond to the right axis (PDI).

3.2. pABOL formulations result in increased protein expression of saRNA *in vivo*

We had previously tested saRNA with formulations with pABOL and LNPs in independent studies for protein and/or vaccine immunogenicity [4–6,11,21,23]. Here, we aimed to test pABOL and LNPs in a head-to-head study to better understand the differences between these saRNA formulations. We formulated saRNA encoding fLuc either with 8 kDa pABOL or 5 different LNP formulations (LM01PE to LM03PC) and quantified the *in vivo* protein expression after 7 days (Fig. 3, Supplementary Fig. 1). We observed that pABOL formulations had significantly higher fLuc expression ($\sim 5 \times 10^6$ p/s) compared to LNP formulations. Within the LNP groups, there was a trend that formulations containing helper lipid DOPE had higher protein expression than those containing DSPC. The DOPE LNP groups ranged from 8×10^4 to 7×10^5 p/s, with LM04PE exhibiting the highest protein expression. Overall, these results indicate that pABOL formulations led to higher intramuscular saRNA translation *in vivo* than LNPs and that within the tested LNP formulations, DOPE enabled superior protein expression compared to DSPC.

3.3. LNP formulations enable higher immunogenicity of saRNA against HA than pABOL

Given the disparity in saRNA protein expression between pABOL and

LNP formulations, we then sought to test how saRNA formulation affects vaccine immunogenicity using influenza hemagglutinin as a model antigen (Fig. 4). We injected mice IM with 1 μ g of saRNA encoding HA from the Cal/09 influenza virus, formulated with the same formulations as the *in vivo* protein expression experiments, and quantified the circulating IgG antibody titers (Fig. 4A). We observed that despite pABOL inducing higher protein expression, the LNP formulations resulted in higher vaccine immunogenicity. Notably, LM03PE resulted in HA IgG levels of $\sim 10^7$ ng/mL at the 6-week timepoint, whereas LM01PE, LM02PE, LM04PE and LM03PC antibody levels were at approximately 10^6 ng/mL and pABOL antibody levels were at $\sim 10^5$ ng/mL. Interestingly, all formulations resulted in approximately equivalent antibody titers ($\sim 10^4$ ng/mL) after a single dose, but there were marked differences after the second vaccination. However, only the titers achieved with LM03PE and LM04PE were statistically significantly higher than those achieved with pABOL at week 6.

We then sought to determine whether the higher antibody titers observed after vaccination with saRNA LNP formulations resulted in increased protective capacity from viral challenge (Fig. 4B). All groups vaccinated with LNP formulations exhibited minimal weight loss, with LM03PC and LM04PE groups exhibiting slightly more weight loss than LM01PE, LM02PE and LM03PE. The group vaccinated with pABOL-formulated saRNA exhibited slightly more weight loss than the LNPs, $\sim 10\%$ after 4 days, but all the mice were partially protected and fully

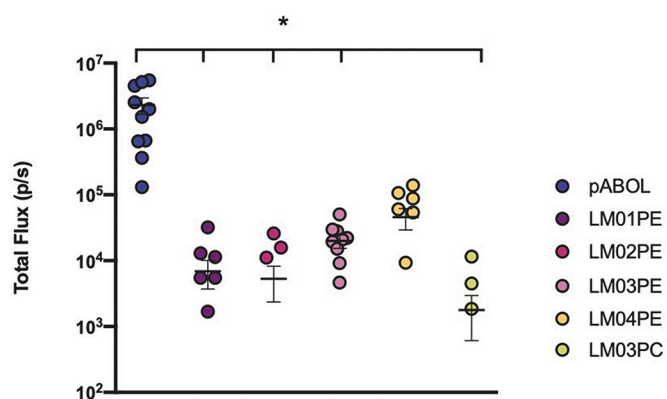


Fig. 3. Effect of polymeric and lipid nanoparticle formulations on saRNA protein expression *in vivo*. Quantification of fLuc expression from pABOL or LNP (LM01PE–LM03PC) 7 days after injection. Mice were injected intramuscularly with 5 μ g of saRNA with an N:P ratio of 45:1 for pABOL and 8:1 for the LNP. For imaging, mice were injected IP with D-luciferin substrate, allowed to rest for 10 min, anesthetized using isoflurane and imaged on an *In Vivo* Imaging System (IVIS) FX Pro as described in the Methods section. Each circle represents one leg of one animal, and line represents mean \pm SD, $n = 5$. *Indicates significance of $p < 0.05$ compared to pABOL as determined by a Kruskal-Wallis test adjusted for multiple comparisons.

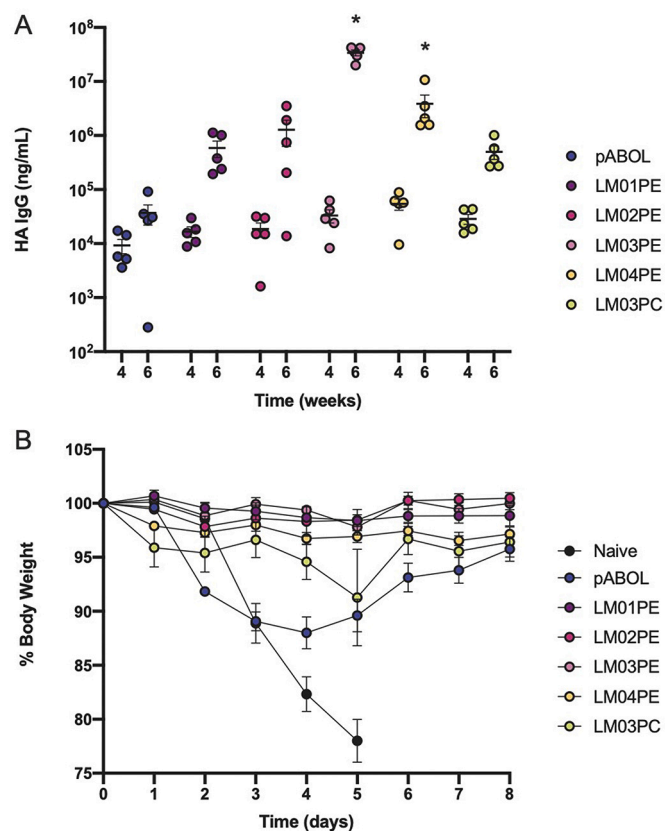


Fig. 4. Immunogenicity of pABOL and LNP formulations against influenza HA (Cal/09). (A) HA antigen-specific IgG antibody titers following IM immunization with a prime and boost of saRNA formulated with pABOL or LNP (LM01PE–LM03PC). Line represents mean \pm SD for $n = 5$. (B) Change in body weight after IN challenge with Cal/09 flu virus for either mice injected IM with pABOL or LNP formulations, or naïve mice. Dots represent mean percentage of body weight normalized to day 0 for each mouse, \pm SD for $n = 5$. *Indicates significance of $p < 0.05$ compared to pABOL as determined by a Kruskal-Wallis test adjusted for multiple comparisons.

recovered. The naïve mice group had significant weight loss that resulted in all mice meeting the humane end point by day 5. Overall, we observed that LNP formulations, especially LM03PE, exhibited higher systemic antibody titers and protection against influenza challenges than the pABOL formulation.

3.4. IM and IN inoculation of saRNA LNP formulations result in both systemic and mucosal SARS-CoV-2 specific IgG

Given the potency of the LM03PE formulations tested in the influenza immunogenicity, we next sought to characterize the dose response curve for LM03PE LNP and compare IM and IN routes of administration. Using the spike glycoprotein from SARS-CoV-2 as a model antigen, given that there may be advantages of IN administration for upper respiratory infections and/or patient preferences, we formulated doses of 0.0001 to 1 μ g of SARS-CoV-2 spike-encoding saRNA in LM03PE LNP, and compared these groups to 1 μ g pABOL injected IM, 1 μ g LM03PE LNP administered IN, and a naïve group (Fig. 5). We then measured the systemic antibody titers at 4 and 6 weeks (Fig. 5A). We observed that 1 μ g of LM03PE LNP administered IM had potent IgG responses of $\sim 10^6$ ng/mL, compared to 1 μ g of pABOL-formulated saRNA which resulted in antibody titers of $\sim 10^3$ ng/mL at 6 weeks. The IM LNP groups exhibited a linear dose response and the lowest group, which received just 0.0001 μ g (0.1 ng of saRNA) exhibiting equivalent antibody titers to 1 μ g of saRNA formulated with pABOL. Encouragingly, we also observed systemic antibody titers for the group that received 1 μ g of LNP IN, although the systemic IgG levels were two orders of magnitude lower than the IM injection of the same dose. The mucosal IgG levels directly mirrored the systemic antibody levels (Fig. 5B), and hardly any mucosal antigen-specific antibody was detected in the 0.0001 μ g IM LNP and pABOL groups.

We also characterized the functionality of the antibody responses by analyzing sera of vaccinated mice using a SARS-CoV-2 pseudotyped viral neutralization assay (Fig. 5C). Again, the results mirror the systemic IgG titers; the 1 and 0.1 μ g groups had the highest IC_{50} levels ($\sim 5 \times 10^3$), whereas there was negligible neutralization from the 0.0001 μ g IM LNP, pABOL and naïve groups. The group that received 1 μ g LNP IN had an appreciable IC_{50} of $\sim 5 \times 10^2$, indicating that this route of administration may be clinically viable. These results show the potency of LNP as a vaccine delivery platform compared to pABOL, and that IN administration may be a viable option.

3.5. LNP formulations induce robust cellular responses against SARS-CoV-2 compared to pABOL formulation

Given the promising humoral responses of the LNP, we also sought to determine how the formulation (LNP vs. pABOL) and route of administration (IM vs. IN) affected the cellular immunity. We re-stimulated splenocytes with SARS-CoV-2 peptides 6 weeks after the initial vaccination and two weeks after a boost, and analyzed the IFN- γ secretion using ELISpot™ (Fig. 6). Similar to the humoral responses, cellular responses were remarkably high in the IM LNP groups, with doses of 1, 0.1 and 0.01 μ g resulting in ~ 1000 SFU/ 10^6 splenocytes. The 0.001 μ g IM LNP, 1 μ g IN LNP and 1 μ g pABOL groups had equivalent responses of ~ 250 SFU/ 10^6 splenocytes, with negligible responses from the 0.0001 μ g LNP and naïve groups. These results show that the IM LNP formulations of saRNA induce superior cellular immunity compared to pABOL and IN inoculation.

3.6. LNPs induce superior Th2 activation and reactogenicity compared to pABOL

In order to probe why the LNP formulations resulted in higher vaccine immunogenicity despite pABOL inducing significantly higher protein expression, we sought to compare the reactogenicity of these formulations. In order to characterize reactogenicity, we analyzed the

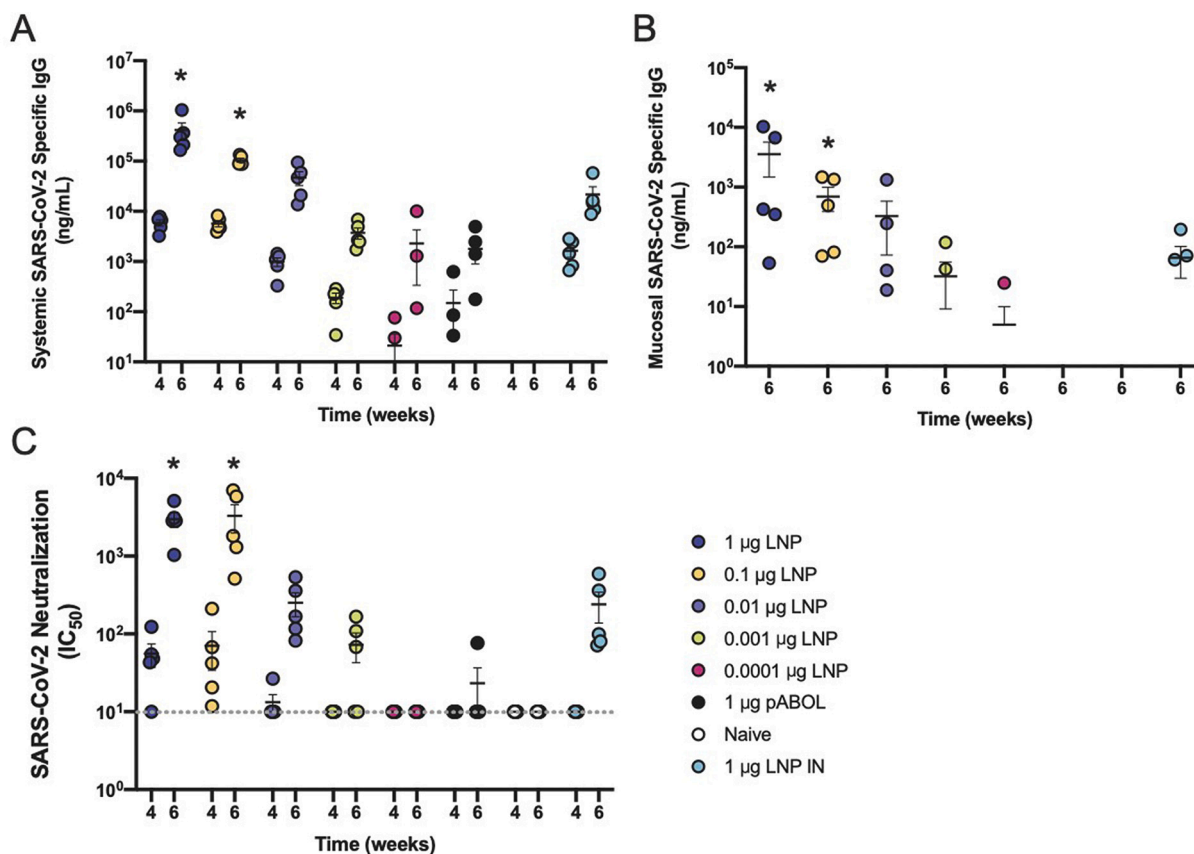


Fig. 5. Dose titration and systemic and mucosal humoral immunogenicity of pABOL and LNP formulations against SARS-CoV-2 after IM or IN inoculation. (A,B) Systemic (A) or mucosal (B) SARS-CoV-2 spike antigen-specific IgG antibody titers following IM or IN immunization with a prime and boost of saRNA formulated with pABOL or LNP (LM03PE). Line represents mean \pm SD for $n = 5$. (C) Neutralization IC_{50} against pseudotyped SARS-CoV-2 virus following IM or IN immunization with a prime and boost of saRNA formulated with pABOL or LNP (LM03PE). Line represents mean \pm SD for $n = 5$. *Indicates significance of $p < 0.05$ compared to pABOL as determined by a Kruskal-Wallis test adjusted for multiple comparisons.

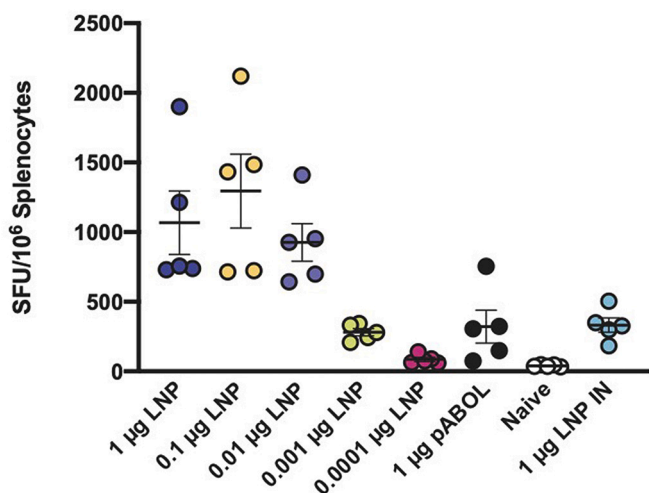


Fig. 6. Cellular immunogenicity to SARS-CoV-2 after prime and boost of saRNA formulated with pABOL or LNP. Quantification of IFN- γ secretion by splenocytes upon restimulation with SARS-CoV-2 peptides, expressed as spot forming units (SFU) per 10^6 cells. Naive animals were used as a negative control. Line represents mean \pm SD for $n = 5$.

sera of mice 4 h after injection with IM LNP/pABOL or IN LNP formulations using a Th1/Th2 cytokine panel (Fig. 7), that included GM-CSF, IFN- γ , IL-1 β , IL-2, IL-4, IL-5, IL-6, IL-12 (p70), IL-13, IL-18 and TNF- α .

We observed that all vaccine formulations resulted in slightly elevated IFN- γ , IL-12, IL-5, and TNF- α compared to the naïve controls, but these results were not statistically significant. However, LNP IM and IN, and pABOL IM formulations did exhibit higher levels of IL-4 (~ 1 pg/mL), whereas there was none detectable for the naïve group (lower limit of detection (LLOD) = 0.05 pg/mL). There was a major difference between levels of IL-6 for the LNP IM group (~ 200 pg/mL) and the LNP IN, pABOL and naïve groups (~ 1 pg/mL). There was no detectable GM-CSF, IL-1 β , IL-2, IL-13 or IL-18 in these samples (data not shown). These data indicate that saRNA formulation and route of administration can cause acute, cytokine-driven reactivity that ultimately enable potent humoral and cellular responses.

4. Discussion

Here, we characterized how polyplex and LNP formulations of saRNA affect both protein expression and vaccine immunogenicity *in vivo* in mice. We observed that pABOL, a bioreducible polymer, yielded higher protein expression than all the LNP formulations tested in these studies. However, the LNP formulations, especially LM03PE, resulted in higher humoral and cellular immunity to two different model antigens, influenza hemagglutinin and the spike glycoprotein of SARS-CoV-2. Within the LNP formulations, those with the phospholipid component DOPE had enhanced immunogenicity over those that had DSPC. We compared how the IM or IN route of administration affected LNP immunogenicity and found that both inoculation routes resulted in systemic and mucosal antibodies, although in each case the antibody titers were an order of magnitude higher with IM injections. We assessed

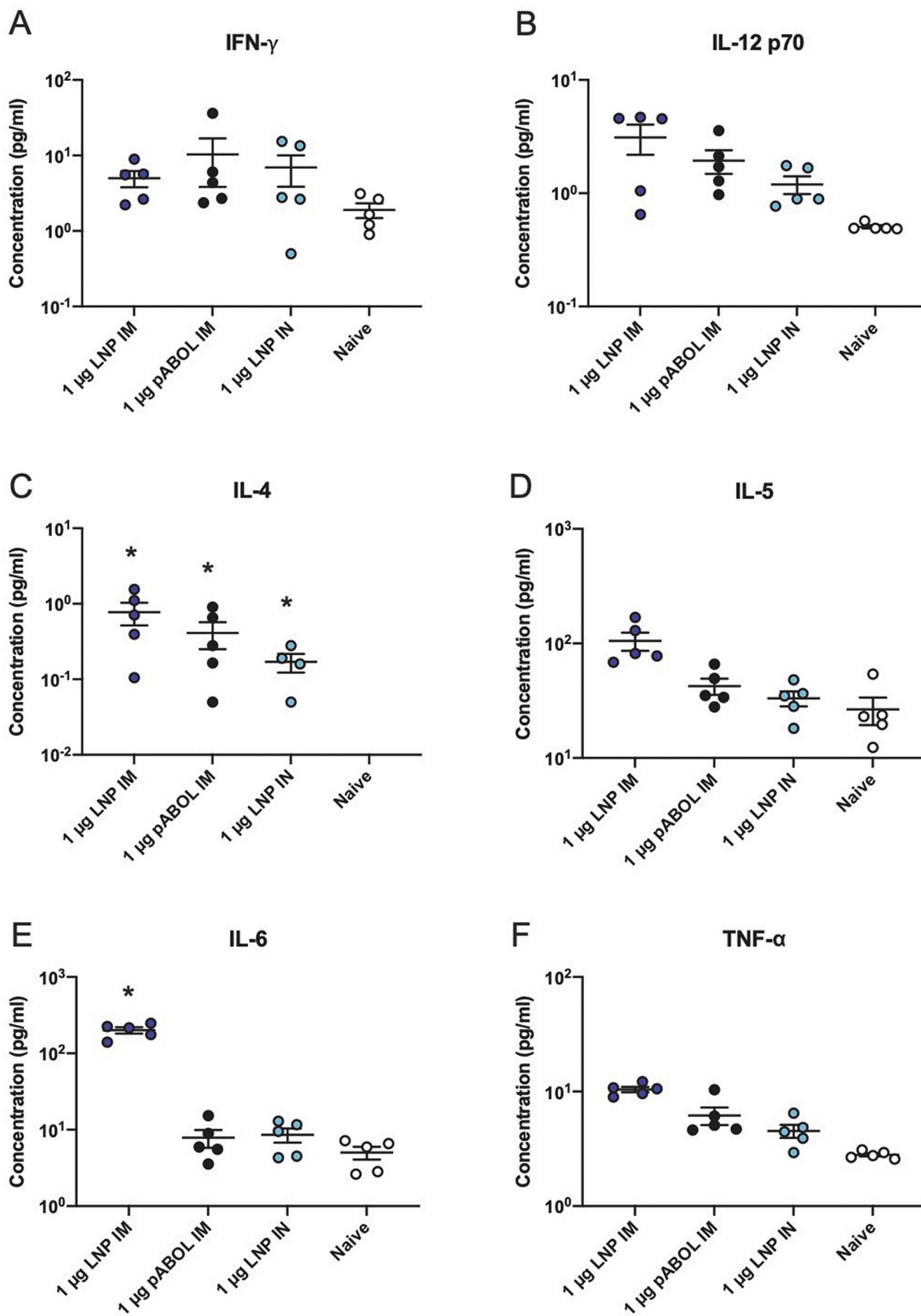


Fig. 7. Cytokine profile in sera of mice 4 h after immunization with saRNA formulated with pABOL or LNP and administered IM or IN. Line represents mean \pm SD for $n = 5$. * indicates significance of $p < 0.05$ compared to naive control as determined by a Kruskal-Wallis test.

the acute systemic cytokine response to pABOL, IM and IN LNP saRNA vaccines and found a significant increase in IL-6 expression with the IM LNP formulation, which could be a contributing factor to the augmented immunogenicity.

Although the size of the pABOL polyplexes and LNP were equivalent (~80 nm, Fig. 2A), there were slight differences in the overall zeta potential of the particles (Fig. 2B). The pABOL particles had a positive surface charge, likely due to the relatively high N:P ratio, which was optimized previously for these formulations [4]. On the other hand, the LNP formulations had a neutral surface charge, as expected for ionizable and PEGylated lipids, and is commonly the case for mRNA and saRNA LNP formulations [6,24]. The differences in surface charge could have had an impact on the immunogenicity, as it has previously been shown that LNP charge can govern biodistribution [25]. However, investigating the biodistribution to different tissues and local protein expression was beyond the scope of this study. Within the tested LNP formulations, we observed that LM04PE has the highest protein expression, but LM03PE was the most immunogenic for both model antigens. Interestingly, the formulation with DSPC (LM03PC) had both lower protein expression and lower immunogenicity than its DOPE counterpart (LM03PE). We hypothesize that the helper lipid in this case also affected the biodistribution of the LNP, as DOPE and DSPC have previously been observed to lead to preferential liver and spleen delivery, respectively, although this was after intravenous administration [26].

To our knowledge, this is the first head-to-head comparison of leading saRNA formulations (polyplex and LNP) to characterize both the protein expression and immunogenicity. Interestingly, pABOL resulted in higher protein expression, whereas LNP resulted in higher humoral and cellular immunity. This indicates that intramuscular antigen expression is not the only factor that affects vaccine immunogenicity, but also that protein expression alone is a poor predictor of vaccine effectiveness. All LNP formulations exhibited higher antibody titres than pABOL at 6 weeks. Among the LNP formulations, LM03PE exhibited the highest systemic antibody titres. Overall, both LNP formulations and pABOL protected against the influenza challenge. It is interesting to note that all LNPs provided complete protection, whereas the mice in the pABOL group exhibited some weight loss, indicative of delayed protection. This may be due to the differences in the antibody titres observed (lower level of antibody titres than LNPs) at week 6. We tested whether IN administration of LNP was a viable inoculation method, and observed both systemic and mucosal antigen-specific, neutralizing antibody responses. This may be an advantageous route of administration for upper respiratory infections, like COVID-19, as has been recently observed with other vaccine platforms (ChAdOx) [27].

While the innate sensing of RNA is well-understood, the innate sensing of delivery vehicles has largely been under investigated. Here, we show that pABOL and LNP formulations both induce elevated levels of IFN- γ , IL-12, IL-5, and TNF- α 4 h after administration (Fig. 7). However, LNP with IM administration resulted in significantly higher levels of IL-6, whereas pABOL and LNP administered IN were equivalent to the control group. This increase in IL-6 has been previously observed for mRNA LNP vaccines [21,28], and may account for the differences observed in downstream immunogenicity. These experiments show that different delivery platforms are advantageous for different niches of saRNA applications; and that while LNP are more potent saRNA vaccine formulations, pABOL formulations resulted in higher protein expression and thus may be more suitable for protein replacement therapies. In addition, these comparative studies highlight the importance of considering the effects of immune sensing of biomaterials, in addition to saRNA, on formulation efficacy.

Author contributions

AKB, PFM, AG and RJS conceived of the study design. NJ and AT conceptualized, designed and synthesized lipids, and designed initial

bio-chemical assays. JY, YZ and MMS designed and synthesized the cationic polymer. NJ carried out bio-chemical assays. AT conceptualized formulation and functional activity studies enabling the selection of lipids for the study. AB carried out early functional activity studies, selection of lipids, and prepared the lipid formulations and formulation protocols. AKB, PFM, KS and KH performed the *in vivo* and *in vitro* experiments. AKB analyzed the data and wrote the manuscript with constructive feedback from PFM, KS, KH, AT, NJ, AB, JY, MMS, AG and RJS.

Declaration of Competing Interest

The authors declare the following competing financial interest(s): AKB, YZ, RJS, and MMS are co-inventors on a patent resulting from this work. AT, NJ and AG are employees of Precision NanoSystems, Inc. The remaining authors declare no competing interests.

Acknowledgements

AKB is supported by a Marie Skłodowska Curie Individual Fellowship (No. 794059) and start-up funding provided by The University of British Columbia. PFM, KH, KS, YZ, MMS and RJS are funded by the Department of Health and Social Care using UK Aid funding and is managed by the Engineering and Physical Sciences Research Council (EPSRC), grant number: EP/R013764/1, note: the views expressed in this publication are those of the author(s) and not necessarily those of the Department of Health and Social Care). JY received funding from the European Union's Horizon 2020 research and innovation programme under the Marie Skłodowska-Curie grant agreement (No. 839137).

Appendix A. Supplementary data

Supplementary data to this article can be found online at <https://doi.org/10.1016/j.jconrel.2021.08.029>.

References

- [1] A.K. Blakney, S. Ip, A.J. Geall, An Update on Self-Amplifying mRNA Vaccine Development, *Vaccines*, 9, 2021.
- [2] S. Perri, C.E. Greer, K. Thudium, B. Doe, H. Legg, H. Liu, R.E. Romero, Z. Tang, Q. Bin, T.W. Dubensky, M. Vajdy, G.R. Otten, J.M. Polo, An Alphavirus replicon particle chimera derived from Venezuelan equine encephalitis and Sindbis viruses is a potent gene-based vaccine delivery vector, *J. Virol.* 77 (2003) 10394.
- [3] A.B. Vogel, L. Lambert, E. Kinnear, D. Busse, S. Erbar, K.C. Reuter, L. Wicke, M. Perkovic, T. Beissert, H. Haas, S.T. Reece, U. Sahin, J.S. Tregoning, Self-amplifying RNA vaccines give equivalent protection against influenza to mRNA vaccines but at much lower doses, *Mol. Ther.* 26 (2018) 446–455.
- [4] A.K. Blakney, Y. Zhu, P.F. McKay, C.R. Bouton, J. Yeow, J. Tang, K. Hu, K. Samnuan, C.L. Grigsby, R.J. Shattock, M.M. Stevens, Big Is Beautiful: Enhanced saRNA Delivery and Immunogenicity by a Higher Molecular Weight, Bioreducible, Cationic Polymer, *ACS Nano*, 2020.
- [5] A.K. Blakney, P.F. McKay, D. Christensen, B.I. Yus, Y. Aldon, F. Follmann, R. J. Shattock, Effects of cationic adjuvant formulation particle type, fluidity and immunomodulators on delivery and immunogenicity of saRNA, *J. Control. Release* 304 (2019) 65–74.
- [6] A.K. Blakney, P.F. McKay, B.I. Yus, Y. Aldon, R.J. Shattock, Inside out: optimization of lipid nanoparticle formulations for exterior complexation and *in vivo* delivery of saRNA, *Gene Ther.* 26 (2019) 363–372.
- [7] L.A. Brito, M. Chan, C.A. Shaw, A. Hekele, T. Carsillo, M. Schaefer, J. Archer, A. Seubert, G.R. Otten, C.W. Beard, A.K. Dey, A. Lilja, N.M. Valiante, P.W. Mason, C.W. Mandl, S.W. Barnett, P.R. Dormitzer, J.B. Ulmer, M. Singh, D.T. O'Hagan, A. J. Geall, A cationic Nanoemulsion for the delivery of next-generation RNA vaccines, *Mol. Ther.* 22 (2014) 2118–2129.
- [8] J.S. Chahal, O.F. Khan, C.L. Cooper, J.S. McPartlan, J.K. Tsosie, L.D. Tilley, S. M. Sidik, S. Lourido, R. Langer, S. Bavari, H.L. Ploegh, D.G. Anderson, Dendrimer-RNA nanoparticles generate protective immunity against lethal Ebola, H1N1 influenza, and *Toxoplasma gondii* challenges with a single dose, *Proc. Natl. Acad. Sci.* 113 (2016), E4133.
- [9] A.J. Geall, A. Verma, G.R. Otten, C.A. Shaw, A. Hekele, K. Banerjee, Y. Cu, C. W. Beard, L.A. Brito, T. Krucker, D.T. O'Hagan, M. Singh, P.W. Mason, N. M. Valiante, P.R. Dormitzer, S.W. Barnett, R. Rappuoli, J.B. Ulmer, C.W. Mandl, Nonviral delivery of self-amplifying RNA vaccines, *Proc. Natl. Acad. Sci. U. S. A.* 109 (2012) 14604–14609.
- [10] P.F. McKay, K. Hu, A.K. Blakney, K. Samnuan, C.R. Bouton, P. Rogers, K. Polra, P.J. C. Lin, C. Barbosa, Y. Tam, R.J. Shattock, Self-amplifying RNA SARS-CoV-2 lipid

- nanoparticle vaccine induces equivalent preclinical antibody titers and viral neutralization to recovered COVID-19 patients, *bioRxiv* 11 (1) (2020) 1–7, 2020.2004.2022.055608.
- [11] A.K. Blakney, P.F. McKay, B. Ibarzo Yus, J.E. Hunter, E.A. Dex, R.J. Shattock, The skin you are in: design-of-experiments optimization of lipid nanoparticle self-amplifying RNA formulations in human skin explants, *ACS Nano* 13 (2019) 5920–5930.
- [12] F.P. Polack, S.J. Thomas, N. Kitchin, J. Absalon, A. Gurtman, S. Lockhart, J. L. Perez, G. Pérez Marc, E.D. Moreira, C. Zerbini, R. Bailey, K.A. Swanson, S. Roychoudhury, K. Koury, P. Li, W.V. Kalina, D. Cooper, R.W. Frenck, L. L. Hammitt, Ö. Türeci, H. Nell, A. Schaefer, S. Ünal, D.B. Tresnan, S. Mather, P. R. Dormitzer, U. Şahin, K.U. Jansen, W.C. Gruber, Safety and efficacy of the BNT162b2 mRNA Covid-19 vaccine, *N. Engl. J. Med.* 383 (2020) 2603–2615.
- [13] L.A. Jackson, E.J. Anderson, N.G. Rounphael, P.C. Roberts, M. Makhene, R.N. Coler, M.P. McCullough, J.D. Chappell, M.R. Denison, L.J. Stevens, A.J. Pruijssers, A. McDermott, B. Flach, N.A. Doria-Rose, K.S. Corbett, K.M. Morabito, S. O'Dell, S. D. Schmidt, P.A. Swanson 2nd, M. Padilla, J.R. Mascola, K.M. Neuzil, H. Bennett, W. Sun, E. Peters, M. Makowski, J. Albert, K. Cross, W. Buchanan, R. Pikaart-Tautges, J.E. Ledgerwood, B.S. Graham, J.H. Beigel, An mRNA vaccine against SARS-CoV-2 - preliminary report, *N Engl J Med* 383 (2020) 1920–1931.
- [14] P.R. Cullis, M.J. Hope, Lipid nanoparticle Systems for Enabling Gene Therapies, *Mol. Ther.* 25 (2017) 1467–1475.
- [15] N. Pardi, M.J. Hogan, F.W. Porter, D. Weissman, mRNA vaccines — a new era in vaccinology, *Nat. Rev. Drug Discov.* 17 (2018) 261–279.
- [16] T. Pepini, A.-M. Pulichino, T. Carsillo, A.L. Carlson, F. Sari-Sarraf, K. Ramsauer, J. C. Debasitis, G. Maruggi, G.R. Otten, A.J. Geall, D. Yu, J.B. Ulmer, C. Iavarone, Induction of an IFN-mediated antiviral response by a self-amplifying RNA vaccine: implications for vaccine design, *The Journal of Immunology Author Choice* 198 (2017) 4012–4024.
- [17] K.J. Kallen, R. Heidenreich, M. Schnee, B. Petsch, T. Schlake, A. Thess, P. Baumhof, B. Scheel, S.D. Koch, M. Fotin-Mleczek, A novel, disruptive vaccination technology: self-adjuvanted RnActive® vaccines, *Hum Vaccin Immunother* 9 (2013) 2263–2276.
- [18] C. de Haro, R. Méndez, J. Santoyo, The eIF-2 α kinases and the control of protein synthesis, *FASEB J.* 10 (1996) 1378–1387.
- [19] S.-L. Liang, D. Quirk, A. Zhou, RNase L: its biological roles and regulation, *IUBMB Life* 58 (2006) 508–514.
- [20] N. Pardi, S. Tuyishime, H. Muramatsu, K. Kariko, B.L. Mui, Y.K. Tam, T.D. Madden, M.J. Hope, D. Weissman, Expression kinetics of nucleoside-modified mRNA delivered in lipid nanoparticles to mice by various routes, *J. Control. Release* 217 (2015) 345–351.
- [21] P.F. McKay, K. Hu, A.K. Blakney, K. Samnuan, J.C. Brown, R. Penn, J. Zhou, C. R. Bouton, P. Rogers, K. Polra, P.J.C. Lin, C. Barbosa, Y.K. Tam, W.S. Barclay, R. J. Shattock, Self-amplifying RNA SARS-CoV-2 lipid nanoparticle vaccine candidate induces high neutralizing antibody titers in mice, *Nat. Commun.* 11 (2020) 3523.
- [22] A. Badamchi-Zadeh, P.F. McKay, M.J. Holland, W. Paes, A. Brzozowski, C. Lacey, F. Follmann, J.S. Tregoning, R.J. Shattock, Intramuscular immunisation with chlamydial proteins induces Chlamydia trachomatis specific ocular antibodies, *PLoS One* 10 (2015), e0141209.
- [23] A.K. Blakney, P.F. McKay, C.R. Bouton, K. Hu, K. Samnuan, R.J. Shattock, Innate Inhibiting Proteins Enhance Expression and Immunogenicity of Self-Amplifying RNA, In Press, *Mol. Ther.* 2020.
- [24] W. Ho, M. Gao, F. Li, Z. Li, X.-Q. Zhang, X. Xu, Next-generation vaccines: nanoparticle-mediated DNA and mRNA delivery, *Advanced Healthcare Materials*, n/a 2001812 (2021).
- [25] L.M. Kranz, M. Diken, H. Haas, S. Kreiter, C. Loquai, K.C. Reuter, M. Meng, D. Fritz, F. Vascotto, H. Hefesha, C. Grunwitz, M. Vormehr, Y. Hüseemann, A. Selmi, A. N. Kuhn, J. Buck, E. Derhovanessian, R. Rae, S. Attig, J. Diekmann, R. A. Jabulowsky, S. Heesch, J. Hassel, P. Langguth, S. Grabbe, C. Huber, Ö. Türeci, U. Sahin, Systemic RNA delivery to dendritic cells exploits antiviral defence for cancer immunotherapy, *Nature* 534 (2016) 396–401.
- [26] R. Zhang, R. El-Mayta, T.J. Murdoch, C.C. Warzecha, M.M. Billingsley, S. J. Shepherd, N. Gong, L. Wang, J.M. Wilson, D. Lee, M.J. Mitchell, Helper lipid structure influences protein adsorption and delivery of lipid nanoparticles to spleen and liver, *Biomaterials Science* 10 (2021), 2001812.
- [27] N. van Doremalen, J.N. Purushotham, J.E. Schulz, M.G. Holbrook, T. Bushmaker, A. Carmody, J.R. Port, C.K. Yinda, A. Okumura, G. Saturday, F. Amanat, F. Krammer, P.W. Hanley, B.J. Smith, J. Lovaglio, S.L. Anzick, K. Barbian, C. Martens, S. Gilbert, T. Lambe, V.J. Munster, Intranasal ChAdOx1 nCoV-19/AZD1222 vaccination reduces shedding of SARS-CoV-2 D614G in rhesus macaques, *bioRxiv* (2021), <https://doi.org/10.1126/scitranslmed.abb0755> eabh0755, 2021.2001.2009.426058.
- [28] J. Lutz, S. Lazzaro, M. Habbaddine, K.E. Schmidt, P. Baumhof, B.L. Mui, Y.K. Tam, T.D. Madden, M.J. Hope, R. Heidenreich, M. Fotin-Mleczek, Unmodified mRNA in LNPs constitutes a competitive technology for prophylactic vaccines, *npj Vaccines* 2 (2017) 29.